International Journal of Innovative Computing, Information and Control
Volume **8**, Number **10(A)**, October **2012**

ICIC International ©2012 ISSN 1349-4198
pp. 6667–6692

MODULATION TECHNIQUES FOR RFID TRANSCEIVER USING SOFTWARE DEFINED RADIO

Mahammad Abdul Hannan, Muhammad Islam, Salina Abdul Samad and Aini Hussain

Faculty of Engineering and Built Environment
Universiti Kebangsaan Malaysia
Bangi, 43600, Selangor DE, Malaysia
{ hannan; m.islam; salina; aini }@eng.ukm.my

Received July 2011; revised November 2011

Abstract. *This paper presents the fundamental concept on the development of a SDR-based RFID simulation model under various modulation techniques. The model efficiently evaluates the performance of multi-array PSK, high data rate QAM and PSAM schemes. The performance of these modulation techniques is evaluated when the system is subjected to a number of users as well as to noise and interference in the channel. AWGN and multipath Rayleigh fading are considered in the channel. The system is analyzed using bit error rate (BER) and signal noise ratio (SNR) for aforesaid modulation techniques and different roll-off factor. The simulation results show a possible solution for future software defined radio in various wireless communication systems. The degradation was also verified with a larger roll-off factor. Additionally, experimental results showed that the PSAM transceiver achieved a high level of data transmission accurately. Two case studies have been conducted to prove the proposed SDR influence on data and image transmission for improving BER performance and image constellation. Finally, a comparison has been made between the proposed and existing SDR systems to analyze and demonstrate the effectiveness of the SDR performance.*
Keywords: Software defined radio, RFID, QAM, PSK, PSAM, Bit-error-ratio, Signal-noise-radio

1. **Introduction.** The rapid growth in RFID communications has shown that wireless communication is viable for data service [1, 2]. Traditional wireless devices are designed to deliver a single communication service using a particular standard. With the steady increase of new wireless services and standards, single purpose devices with dedicated hardware resources can no longer meet the users' needs. It is also expensive to upgrade and maintain a wireless system each time a new standard comes into existence [3].

A feasible solution to make communication systems more flexible and user friendly can be achieved through the software defined radio (SDR) concept. SDR refers to the class of reprogrammable or reconfigurable radios in which the same piece of hardware can perform different functions at different times. It has generated tremendous interest in the wireless communication industry because of the wide-ranging economic and deployment benefits it offers [4, 5, 6, 7]. SDR promises to increase flexibility, extend hardware lifetime and costs [8, 9]. It is an advanced radio technology in which the modulation and demodulation of radio signals are performed exclusively by software [10]. Therefore, it reduces the peripheral hardware of the RFID communication devices. The communication link of the SDR mainly consists of the transmitter, channel and receiver [11]. The transmitter processes an information signal to produce a signal most likely to pass reliably and efficiently

through the channel to the receiver. It can find code as close to the antenna as possible, define the transmitted waveforms and demodulate the received waveforms [12, 13, 14].

SDR offers a flexible radio architecture that allows for upgrading and the addition of features to the radio that are easily implemented through the software [15, 16]. Additionally, advanced signal processing techniques involving multiple antennas and phase shift keying (PSK), Quadrature amplitude modulation (QAM) and pilot symbol assisted modulation (PSAM) techniques can easily be implemented without necessitating major hardware changes in the RFID transceiver [17]. The major factors that are expected to create a wider acceptance of reconfigurable radios are limited bandwidth, multi-functionality, global mobility, compactness and power efficiency, ease of manufacture and ease of upgrade [18, 19].

Constant envelope, PSK signals are used to keep signal recovery inexpensive and minimally complicated [9, 20, 21]. Standard PSK constellations are constructed of symbols with equal energy that are evenly distributed about the origin of the normalized unit circle in the complex plane [22, 23]. Modulated envelope, QAM signals are used to improve power efficiency, with added device cost for highly linear amplifiers. With standard QAM, symbols are positioned to form a square lattice in the complex plane. The constellation structures of both of these signals lend themselves to ambiguity in phase and have limited bandwidth to adapt in dynamic environments [24, 25]. QAM yields high spectral efficiency due to its use of amplitude and phase modulation and, therefore, is an effective technique for achieving high channel capacity. The application of QAM for land mobile communication in the presence of a rapidly fading channel is challenging because of the amplitude distortion introduced, thus requiring high quality channel estimation and equalization. Many researchers have studied PSAM to compensate for the fading effects at the receiver [27]. Different communication techniques are used to provide a considerable amount of flexibility while maintaining performance [28, 29]. The performance of modulation techniques in terms of modulation, signal to noise rario, numbers of errors, BER and application, respectively is shown in Table 1 [30, 31, 32].

In SDR, modulation and demodulation of radio signals are performed exclusively by software. Thus, it reduces the peripheral hardware of the RFID communication devices. In the majority of systems proposed in literature, inflexible frequency and limited bandwidth are used for channel capacity due to channel availability, the spectrum to convey information and the cost. SDR based RFID transceivers require limitless bandwidth to communicate the reliability and integrity of the data from source to sink, which can be accomplished by searching for low cost alternatives to the existing SDR. The solution should be accomplished with an acceptable processing of modulation and demodulation with a limitless bandwidth channel. This paper addresses an SDR-based digital signal processing technique to process an RFID signal and provides an evaluation of the system performance by comparing the signal to noise ratio (SNR) versus bit error rate (BER) of the signal using multi-modulation techniques.

With the proliferation of wireless standards future wireless devices would need to support multiple hardware interfaces and modulation formats. Software defined radio (SDR) technology enables such functionality in wireless devices by using reconfigurable hardware platform such as FPGA and DSP across multiple standards. With FPGA and data converter technology continuously evolving, the SDR concept is increasingly becoming a reality. DSP provides greater flexibility and higher performance in terms of attenuation and selectivity as well as reducing manufacturing costs. For example, TriMatrix memory architecture provides a highly flexible and integrated platform to implement computationally intensive digital IF functions including digital up-down converters. The detail enabling features between FPGA chip and DSP chip are shown in Table 2 [33].

TABLE 1. Comparison of SDR system performance

SDR	*Modulation Techniques*	*Signal-to noise Radio*(E_b/N_o)	*Number of Error*	*Bit Error Rate* (*BER*)	*Application*
Wideband Code Division Multi-Access [30]	PSK	5	61.830	6.025000e-003	Satellite, GPS
	QAM	6	51.830	6.183000e-002	Hyper-frequency digital link
	PSAM	6	12.05	5.183000e-002	
Wireless LAN [31]	PSK	6	60.6	6.153000e-002	ERMES, Mobile data, Public Safety
	QAM	7	49.8	6.693000e-002	Modems
	PSAM	8	13.3	5.13000e-002	
High Rate DirectSquence Spread Spectrum [32]	PSK	1	63.2	6.063000e-002	EGPRS
	QAM	2	52.89	6.363000e-002	
	PSAM	5.5	13.55	5.13000e-002	

TABLE 2. A comparison of FPGA and DSP chips

Enabling Language	*FPGA chip*	*DSP chip*
Programming Language	VHDL, Verilog	C, Assembly Language
Ease of Software Programming	Fairly easy. However, a programming is complex	Easy
Performance	Very fast if an appropriate architecture is designed	Limited by the clock speed of a DSP chip
Configurability	SRAM-type FPGAs can be reconfigurable infinite time	Reconfigurable by changing program memory content
Reconfiguration Method	Through downloading configuration data to a chip electronically	Simply reading a program at a different memory address.
Areas where FPGAs can outperform DSPs, etc.	FIR filter, IRR filter, correlator, convolver, FFT, etc.	A signal processing program of sequential nature
Power consumption	Can be minimized or power can be dynamically controlled	Not minimized due to same number of memory chip
Implementation method of MAC	Parallel multiplier/adder or distributed arithmetic	Repeated operation of MAC function
Speed of MAC	Can be fast if a parallel algorithm is used.	Limited speed of MAC operation of a DSP chip
Parallelism	Can be parallelized to achieve high performance	Sequential and cannot be parallelized

2. **Current Challenges and Problems.** Current challenges and problems of the wireless devices or radio transceiver in terms of inflexibility, adaptation and traditional radio design are as follows.

i. Conventional radio technology has a limitation to improve bandwidth and channelization with respect to carrier frequencies. Thus, the limited observability and testability of radio transceivers are the most ticklish matters for radio developer [34].

ii. Some hardware of the joint tactical radio system (JTRS) is a complex processing such as multiple processors and/or FPGAs and software. The complex processing must satisfy contradictory requirements of high computational throughput extremely power sufficient and must be programmable and reprogrammable [10].

iii. Tradition radio designs have low flexibility to adapt to new services and standards. However, if any design parameters changes, radios cannot correctly decode the information under the new conditions. Thus, the system must be redesigned and hardware modules

have to be replaced which imply higher costs and longer time for the development and manufacturing of new products [35, 36].

iv. The functionality of conventional radio architectures is determined by hardware with specific configuration. Thus, the migration of functions from an older version to the new version is not possible in conventional systems [37].

v. A large number of SDR products have been developed for running wireless or RFID devices. However, running SDR on small size, limited weight and long battery life embedded devices are facing constrains and challenges [38, 39].

vi. The general purpose processors and DSPs are relatively flexible and easy to program, but consume high power and are often limited in computational throughput. Field programmable gate arrays (FPGAs) and application specific integrated circuits (ASICs) can deliver extremely high performance, throughput and power-efficiency. However, they are costly and difficult to fabricate with long product development times, and commit the system designer to a hardwired solution that offers little or no re-programmability [40].

Thus, the aim of SDR is to explore new design tools, especially for RFID signals to reduce the amount of hardware, allow rapid development, reducing the amount of time required to stimulate and to transfer the radio signal either ways of the transceiver. In SDR based RFID system a significant amount of signal processing algorithms is performed in software. This interfaces to RFID signal that is generic enough to support a range of frequencies and modulation schemes.

3. **SDR Based RFID Transceiver.** This study involves with the modeling and simulation of the communication channels, BPSK transmission system, QAM transmission system and PSAM transmission system, lastly calculation and comparison of BER and signal to noise ration, respectively. The BER performance for PSK, QAM and PSAM transmission schemes of RFID transceiver is investigated.

A typical wireless communication link includes a transmitter, a communication medium or channel, and a receiver. The ability to simulate all three of these elements is required in order to successfully model any end-to-end communication system. The transmitter and receiver elements can in turn be subdivided into further sub-systems, as shown in Figure 1. These include a data source (analog or digital), an optional data encoder, a modulator, a demodulator, an optional data decoder and a signal sink. The data source generates the information signal that is intended to be sent to a particular receiver. This signal can be either an analog signal such as speech or RFID, or a digital signal such as a binary data sequence. This signal is typically a baseband signal represented by a

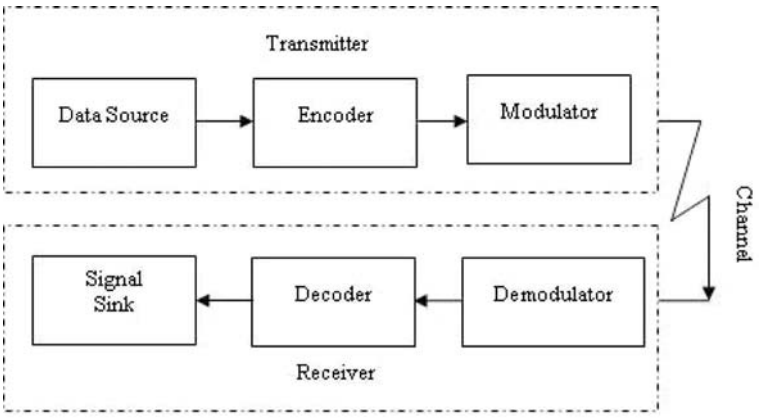

FIGURE 1. Communication system elements

voltage level. For analog signal, it is often desirable digitally encode the signal prior to transmission by undergoing a quantization process. This step converts the analog signal into a digital signal. While some information is lost in this process, the resulting digital signal is often far less susceptible to the effects of noise in the transmission channel.

An encoder can also be used to add redundancy to a digital data stream, in the form of additional data bits, in a way that provides an error correction capacity at the receiver. It is important to note that usually the output bit rate of an encoder is not equal to input bit rate. Properly distinguish between the two bit rates; the transmitter's input rate is referred to as the information data rate, while the transmitter output rate is referred to as the channel data rate.

Depending on the type of information signal and the particular transmission medium, different modulation techniques are employed. Modulation refers to the specific technique used to represent the information signal as it is physically transmitted to the receiver. For example, in PSK, QAM and PSAM, the information is represented by phase or phase and amplitude variations of the carrier signal. Once the signal is modulated, it is sent through a channel to reach the intended receiver. This may be a copper wire, coax cable, or the atmosphere in the case of a radio transmission. To some extent, all channels introduce some form of distortion to the original signal. Many different channel models have been developed mathematically represent such distortions. A commonly used channel model is the Additive White Gaussian Noise (AWGN) channel. In this channel, noise with uniform power spectral density (hence the term "white") is assumed to be added to the information signal. Other types of channels include fading channels and multipath channels.

Once the transmitted signal reaches the intended receiver, it undergoes a demodulation process. This step is the opposite of modulation and refers to the process required to extract the original information signal from the modulated signal. Demodulation also includes any steps associated with signal synchronization, such as the use of phase locked loops in achieving phase coherence between the incoming signal and the receiver's local oscillator. When data encoding is included at the transmitter, a data decoding step must be performed prior to recovering the original data signal. The signal decoding processing is usually more complicated than the encoding process and can be very computationally intensive. Efficient decoding schemes, however, have been developed over the years. One example is the Viterbi decoding algorithm, which is used to decode convolutional encoded data.

Finally, an estimate of the original signal is produced at the output of the receiver. The receiver's output port is sometimes referred to as the signal sink. As communications engineers, we are usually interested in knowing how well the source information was recreated at the receiver's output. Several metrics are used by engineers to evaluate the success of the data transmission. The most common metric, in the case of digital signals, is the received BER. Other valuable performance indicators include the received signal to noise ratio SNR and eye diagram.

4. **Modulation Techniques.**

Many types of modulation techniques have been devised for representing an information signal as it is being transmitted. In general, all modulation schemes rely somehow on varying the amplitude, phase or both of a "carrier" waveform. At a high level, modulation techniques can be subdivided into two basic groups: analog modulation and digital modulation.

4.1. **Analog modulation.**

In analog modulation, the transmitted signal can be varied continuously over a specified range in contrast to assuming a fixed number of predetermined states. Examples of analog modulation techniques include Amplitude Modulation

(AM), Phase Modulation (PM) and Frequency Modulation (FM). As the named implies, an AM transmitter operates by varying the amplitude of the carrier according to the voltage of the input signal. In a PM transmitter, the input signal is used to control the instantaneous phase of the carrier phase. With FM, on the other hand, the input signal is used to vary the instantaneous frequency of the carrier. In all three cases the input signal is an analog signal, such as a voice signal.

4.2. **Digital modulation.** In digital modulation, the transmitted signal can assume only a fixed number of predetermined states, usually referred to as the "alphabet size" or constellation size of the modulation signal. These include discrete amplitude levels, discrete phases, discrete frequencies, or combinations of the above. Examples of digital modulation techniques include PSK, QAM and PSAM. Each of the above techniques can be implemented at various levels of complexity depending primarily on the total number of distinct states (constellation points) which are allowed within the modulator.

Digital modulation has inherent benefits over analog modulation as its distinct transmission states can more easily be detected at a receiver in the presence of noise than an analog signal which can assume an infinite number of values. When the transmitted signal originates as an analog waveform, a tradeoff occurs at the encoding stage since some information is always lost in the quantization process. The example in Figure 2 and Figure 3 shown compare of two digital modulation techniques using an arbitrary digital input signal. The top plot of Figure 2 and Figure 3 showed the random binary input signal. The additional plot showed their corresponding modulator, which showed the difference between the output of a ASK modulator and PSK modulator given the same input signal. Modulation techniques in SDR are presented for three categories of modulation and are analyzed over AWGN and Rayleigh fading channels. The modulations that support the communication system, which allow RFID signals, are PSK, QAM and PSAM.

4.2.1. *Phase shift keying (PSK).* In PSK modulation, the transmitted information over a communication channel is impressed on the phase of the carrier. The phase of the carrier changes between different phases determined by the logic states of the input bit stream. In two-phase shift keying, the carrier assumes one of the two phases. Logic 1 produces no

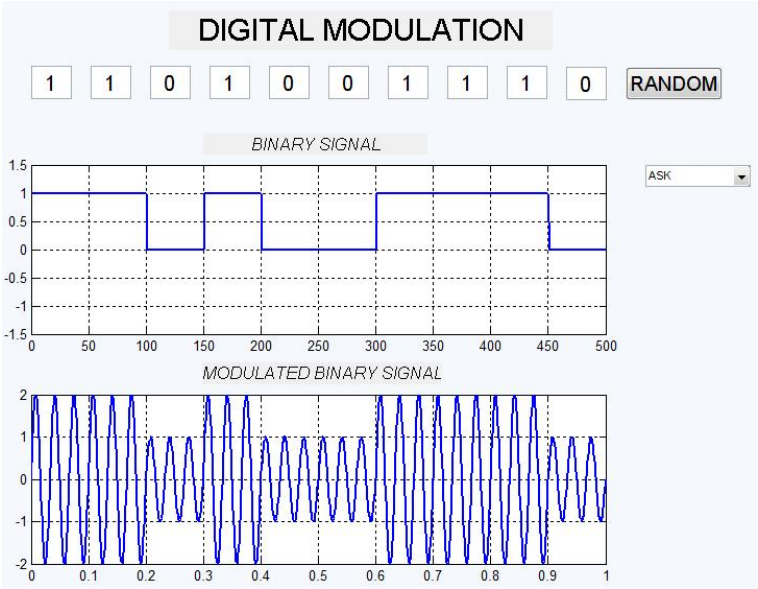

FIGURE 2. ASK digital modulation

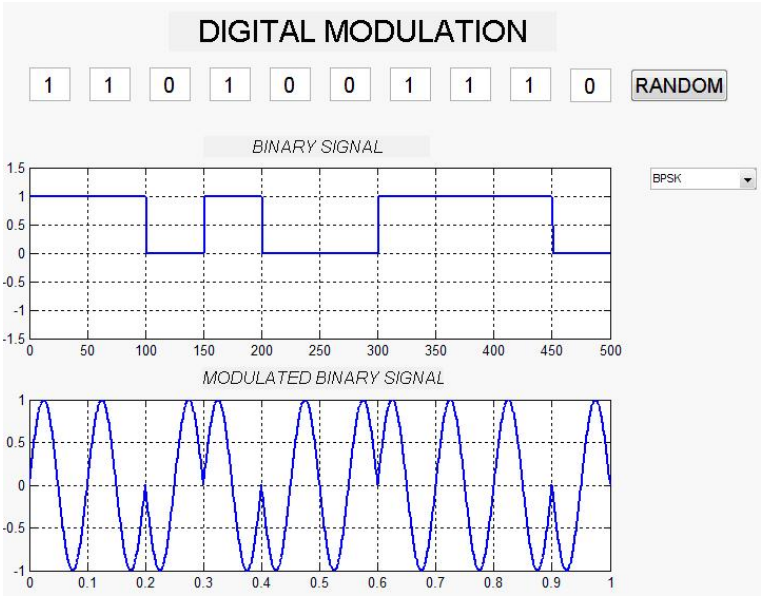

FIGURE 3. PSK digital modulation

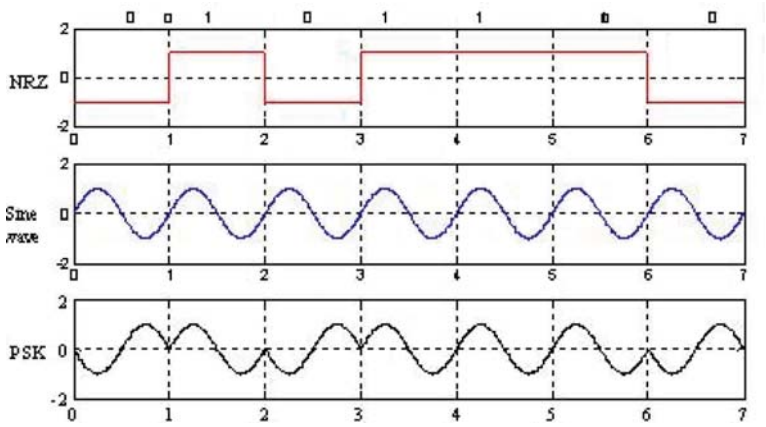

FIGURE 4. PSK waveform from NRZ waveform

phase change and logic 0 produces an 180° phase changes. This modulated signal can be expressed as:

$$s(t) = \begin{cases} A(t)\cos\left(2\pi f_c t + \phi(t)\right) & \text{symbol 0} \\ A(t)\cos\left(2\pi f_c t\right) & \text{symbol 1} \end{cases} \tag{1}$$

where $A(t)$ is the amplitude modulation, (t) is the phase modulation, and f_c is the frequency of the carrier. Information is transmitted by varying the amplitude and the phase of the carrier signal. Figure 4 illustrates the above digital modulation schemes for the case in which the data bits are represented by the polar non-return zero (NRZ) waveform. 4.2.1.1. PSK transceiver system. In this modulation scheme, the input digital data 0 and 1 is directly converted to the phase of 0 and π, respectively. The waveform is shown as follows:

$$s(t) = A(t)\cos\left\{2\pi f_c t + \pi . d_k\right\}, \tag{2}$$

where d_k is the information data sequence.

The waveform of a PSK wave is generated by multiplying between the digital signal data and carrier wave as shown in Figure 5. Prior to that, the generated data are fed into a pulse shaping filter to control the shape. Reasons for this are the limitation of

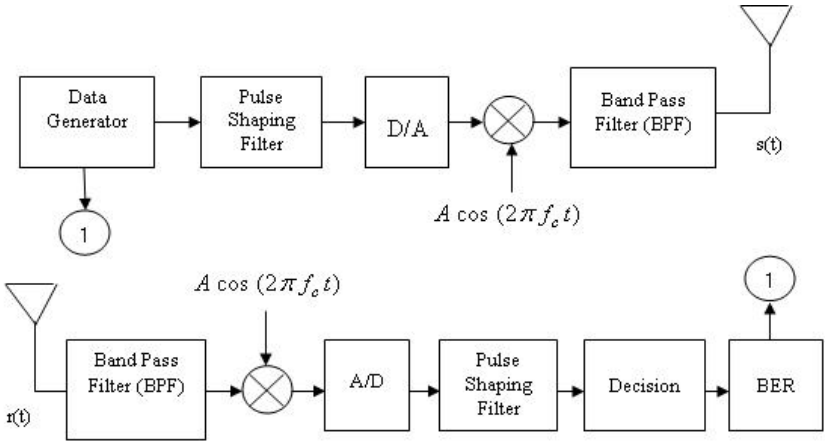

FIGURE 5. Transmitter and receiver of the PSK transmission

the frequency bandwidth and also the reduction of spurious signals. The next section includes the method used for the design of an adequate pulse shaping filter. Then, the pulse-shaped signal is converted to analog signal by a digital to analog (D/A) converter, up converted to the RF frequency by multiplying by the carrier signal wave, and finally transmitted to the air.

At the receiver, the received wave passes a bandpass filter (BPF), where the spurious wave is eliminated. Then, the received signal is down converted to the baseband by multiplying the received radio signal by the RF carrier frequency signal. The signal is subsequently converted to digitally sampled data with an analog to digital (A/D) converter, and the transmission digital data is recovered by DSP hardware. The sampled data is then filtered to eliminate the symbol interference at a pulse shaping filter circuit. Finally, a synchronization point is selected from the filtered digital sampled signal. If the signal is larger than 0 at the point, we can obtain the received digital data 1; otherwise, the received data becomes 0.

4.2.1.2. PSK model. This section explains the mathematical model of a PSK transmission scheme. The transmission digital data sequence is given as:

$$\begin{aligned} d(t) &= \sum_{k=-\infty}^{\infty} d_k.(g_T(t) \times \delta(t - kT_b) \\ &= \sum_{k=-\infty}^{\infty} d_k.g_T(t - kT_b) \end{aligned} \tag{3}$$

where d_k is transmission digital data, g_T is the trailing rectangular pulse of each transmission digital data, and T_b is the bit duration, respectively. The reciprocal of T_b is the bit rate, and $\delta_T(t)$ is delta function:

$$\delta_T(t) = \begin{cases} 1 & t = 0 \\ 0 & \text{otherwise} \end{cases} \tag{4}$$

when $g_T(t)$ is a trailing rectangular pulse,

$$g_T(t) = \begin{cases} 1 & -\frac{T_b}{2} \leq t \leq \frac{T_b}{2} \\ 0 & \text{otherwise} \end{cases} \tag{5}$$

The example given in Figure 6, d_k, $k = 16 = [1, 0, 1, 1, 0, 0]$ and 0 data is converted to -1. While the pulse shape in 6 looks digital (square), from the view point of the frequency domain, the shape radiates large spurious signals for other frequency channels. A square

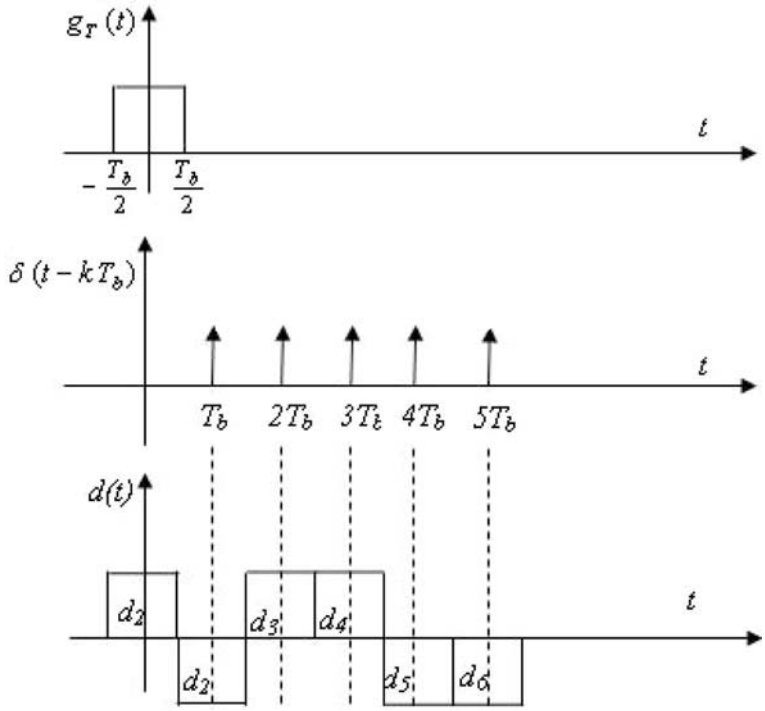

FIGURE 6. Relationships between d_k, $g_T(t)$, $\delta(t)$ and $d(t)$

signal in time domain produces a sine signal in frequency domain and vice versa. Hence, to obtain a nice square signal in frequency domain, the pulse shape in time domain must take the sine function but in this case, spurious signals appear in the area $|t| > T_b/2$. Thus, a filter with adequate optimum shape that reduces the number of spurious signals in the time and frequency domains is needed.

Using (3) and (5), the PSK transmission of the data can be configured. The configured signal is modulated by multiplying the carrier frequency signal $\cos(2\pi f_c t)$ and then transmitted to the air. The transmitted signal is given by:

$$s(t) = d(t)\cos(2\pi f_c t) \tag{6}$$

The transmitted signal is contaminated by multipath fading and AWGN and at the receiver, the signal is as:

$$r(t) = \int_0^\infty h(\tau, t) \times s(t-\tau)d\tau + n(t) \tag{7}$$

where $h(\tau, t)$ is the impulse response of the radio channel at time t, and $n(t)$ is the receiver noise.

In the receiver, the received signal is first filtered by a BPF, which is assumed to have a sufficient passband so that the signal is negligibly distorted. The filtered signal is multiplied by a carrier wave that has same frequency as the transmitter but the initial phase of the carrier signal source is different between the transmitter and receiver. Thus, the carrier signal source at the receiver is mentioned as $\cos\{2\pi f_c t + \theta_1(t)\}$ where $\theta_1(t)$ is the initial phase value of the carrier signal. The multiplied signal is given by:

$$r_2(t) = r(t)\cos\{2\pi f_c t + \theta_1(t)\} \tag{8}$$

where $r(t)$ is given by (8). For simplification, it is assumed no filtering is done at this point, therefore,

$$r(t) = [R(t)d(t)(\cos\theta_f(t) + n_1(t))]\cos(2\pi f_c t) + n_2(t) \tag{9}$$

where $R(t)$ and $\theta_f(t)$ are the time-variant fluctuations of the amplitude and phase respectively by the radio channel. The $n(t)$ is the receiver noise and is expressed as:

$$n(t) = R(t) \times n_1(t) \times \cos(2\pi f_c t) + n_2(t) \tag{10}$$

where $n_1(t)$ and $n_2(t)$ are the noise component around f_c and other noise component, respectively. In addition, the cosine and sin matrix is a rotation matrix with the phase. Using Equations (8) and (9) and LPF is used for the expansion value. Hence, the high frequency signal is eliminated giving the following equation:

$$r_3(t) = \frac{1}{2}(R(t) \times d(t)(\cos\theta_f(t) + n(t))) \times \cos\theta_1(t) \tag{11}$$

Then, Equation (12) is filtered by a pulse shaping, filter-based root Nyquist filter to reduce the ISI.

$$r_4(t) = \frac{1}{2}R(t) \times \cos\theta_f(t) \times \cos\theta_1(t).\sum d_k.(g_T(t) \times g_R(t) \times \delta(t - kT_b)) + n_3(t) \tag{12}$$

Next, the filtered signal is oversampled at a sampling rate of n/T_b (n is an integer) by using an A/D converter. The sampled signal is

$$r_4\left(k.\frac{T_b}{n}\right) \quad k = 0, 1, 2, \ldots \tag{13}$$

When $t = u.T_b/n$ (u is an integer), the maximum value of the pulse from the characteristics of the Nyquist filter can be obtained. A synchronization method must be considered but the purpose of this project, it is assumed that synchronization point is known. Then, Equation (14) is resampled at every T_b or every n sample from the synchronization point.

$$r_4\left(u.\frac{T_b}{n}\right) \tag{14}$$

Finally, the resample data $r_5(t) = r_4(t)(\text{syncpoint} + l.T_b)$, $l = 0, 1, 2, \ldots$ is obtained. The received data can then be decided whether it is a 1 or 0 by using the threshold condition equation:

$$\hat{d_k} = \begin{cases} 1 & (r_5(l) > 0) \\ 0 & (r_5(l) \leq 0) \end{cases} \tag{15}$$

By comparing $\hat{d_k}$ and d_k, the BER, which depends on the receiver noise, can be calculated. Theoretical BER in an AWGN and one-path Rayleigh fading channels have been reported [36, 37].

4.2.1.3. PSK constellation. In PSK constellation, 2 bits are processed to produce a single-phase change. The actual phases are produced by a 4-PSK modulated signal in which a signal space diagram or signal constellation can be drawn as shown in Figure 7(a). Now from the constellation diagram consider any two closest bits sequences, there is only one bit change. This is called Gray Coded scheme. For example, bit sequence 00 has one bit change for its closest bit sequences 01 and 10. However, in 3 bits are processed to produce a single-phase change. This means that each symbol consists of 3 bits. Figure 7(b) shows the constellation and mapping of the 3-bit sequences onto appropriate phase angles. In n-bits of PSK modulation, 16-PSK or 32-PSK or higher orders PSK modulation can be designed and represented on a signal space diagram. Figure 7(c) shows the 4 bits 16-PSK constellation.

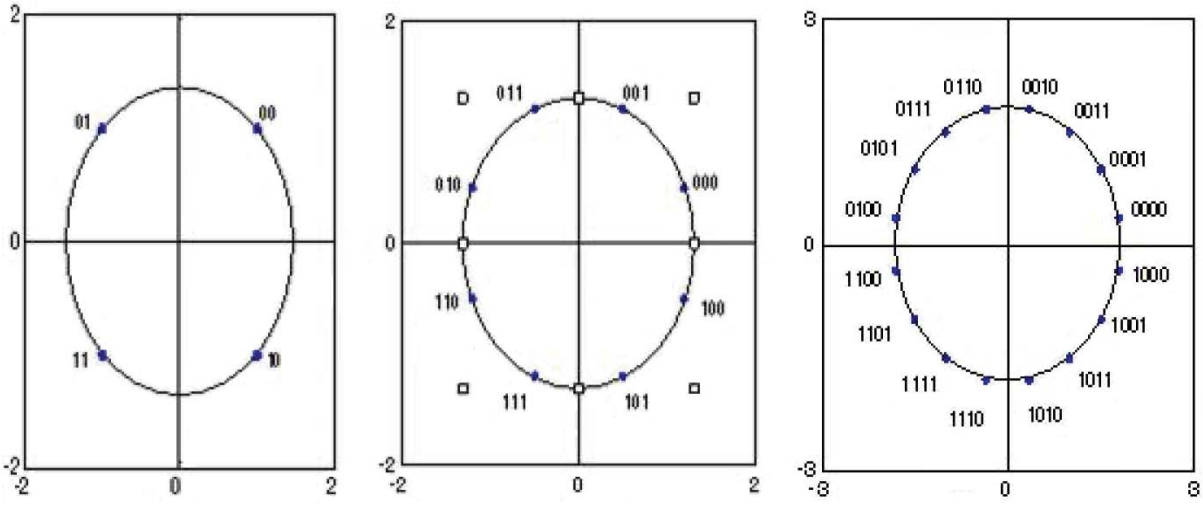

FIGURE 7. 4-PSK, 8-PSK and 16-PSK constellation

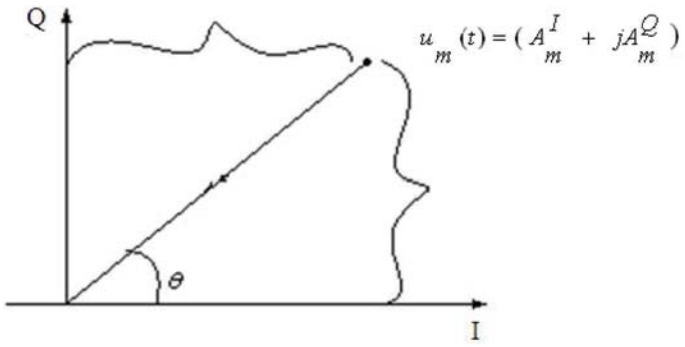

FIGURE 8. IQ constellation diagram

4.2.2. *Quadrature amplitude modulation (QAM).*

4.2.2.1. QAM model. Wireless channels vary over time due to fading and changing interference conditions. Adaptive modulation exploits these variations to maximize the data rate that can be transmitted over such channels in an energy efficient manner. This requires use of spectrally efficient modulation schemes such as QAM. Multilevel QAM makes it possible to achieve high spectral efficiency while employing PSAM based channel estimators. The perfect knowledge of the channel is assumed to examine the effect of delay and Doppler spread on adaptive modulation, and then examines the impact of channel estimation and equalization. QAM is a method for sending two separate channels of information. The carrier is shifted to create two carriers namely the $\sin(2\pi f_c t)$, and $\cos(2\pi f_c t)$ versions. The outputs of both modulators are algebraically summed containing the in-phase I and quadrature Q information. The set of possible combinations of amplitudes on an x-y plot is a pattern of dots known as a QAM constellation as shown in Figure 8.

The baseband equivalent representation, $u_m(t)$, of the QAM signal can be expressed as

$$u_m(t) = \left(A_m^I + jA_m^Q\right) g(t) \quad m = 1, 2, \ldots, M \tag{16}$$

where A_m^I, A_m^Q is a constant of average transmitted power referred to the in-phase, I and quadrature, Q amplitudes corresponding to the M possible symbols in the two-dimensional space. The function $g(t)$ is a real-valued signal whose shape influences the

spectrum of the transmitted signal. The $u_m(t)$, in (20) can also be represented in polar form as follows.

$$u_m(t) = A_m e^{j\theta_m} g(t) \quad m = 1, 2, \ldots, M \tag{17}$$

where A_m and θ_m denote the amplitude and phase of the m^{th} symbol, and are given by

$$\begin{aligned} A_m &= \sqrt{(A_m^I)^2 + \left(A_m^Q\right)^2} \\ & \qquad\qquad m = 1, 2, \ldots, M \\ \theta &= \tan^{-1}\left(\frac{A_m^Q}{A_m^I}\right) \end{aligned} \tag{18}$$

The baseband signal described in (21) can be expressed as a bandpass signal, $S_m(t)$, which is chosen from one of M possible signaling waveforms as follows.

$$s_m(t) = \text{Re}\left(u_m(t)e^{j2\pi f_c t}\right) \quad m = 1, 2, \ldots, M \tag{19}$$

where f_c is the intermediate carrier frequency. Alternatively, the bandpass QAM signal in (21) can be expressed equivalently in terms of its quadrature components as

$$\begin{aligned} &s_m(t) = A_m^I \cos(2\pi f_c t) - A_m^Q \sin(2\pi f_c t) \\ &0 \le t \le T \quad m = 1, 2, \ldots, M \end{aligned} \tag{20}$$

where $A_m^I = A_m g(t)\cos(\theta_m)$ and $A_m^Q = A_m g(t)\sin(\theta_m)$.

QAM is designed to transmit two separate signals independently with the same carrier frequency by using two quadrature carriers. These two separate modulated signals are then added and transmitted. This structure of QAM allows for M discrete amplitude levels (M-QAM), and thus permits a symbol to contain more than one bit of information. The general form a M-QAM signal is given by Equation (20), where $g(t)$ is the signal pulse shape, A_m^I and A_m^Q are the information bearing signal amplitudes of the quadrature carriers. This representation leads to the most common functional representation of the QAM modulator, which is shown in Figure 9.

The input baseband sequence with bit rate R_b bits/second is encoded into two quadrature M level pulse amplitude modulation (PAM) signals, each having a symbol rate of $R = R/K$ symbols/second $K = \log_2(M)$. These two components of I and Q are then filtered by pulse-shaping lowpass filters (LPF's) $g(t)$, to limit the transmission bandwidth. Finally, the quadrature signals modulate the I and Q carrier's for transmission. The

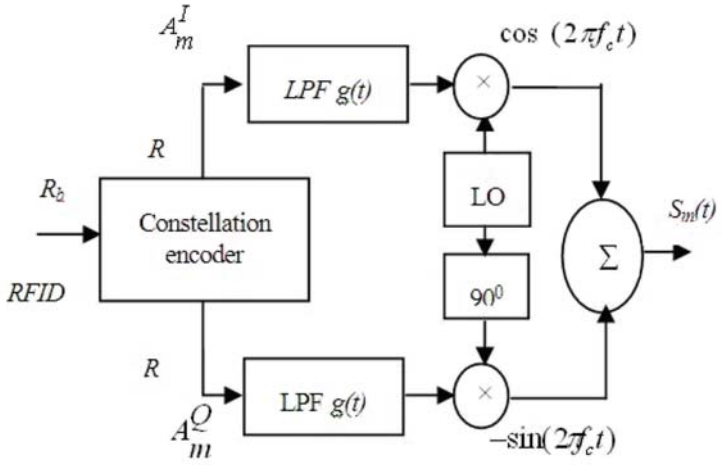

FIGURE 9. QAM modulator

transmitted bandpass signal $s_m(t)$, which is the summation of all symbols represented by the M possible signaling waveforms for QAM, can be expressed as:

$$s_m(t) = \mathrm{Re}\left\{\sum\nolimits_n I_n g(t - nT) e^{j2\pi f_c t}\right\} \tag{21}$$

where transmission rate is $R = 1/T$ symbols/second and I_n represents the discrete information bearing sequence of symbols and is complex valued for QAM. Since the modulator output frequency is often lower than the desired transmission frequency, the modulator frequency must be up-converted to the appropriate radio frequency (RF) for transmission.

4.2.2.2. QAM constellation. QAM is standardized in terms of the number of M of discrete levels number which is chosen to be a power of 2 so that each symbol can be separated by a specific number of bits. QAM transmits bits of information during each symbol period. For 16-QAM, there are 16 possible symbols each containing 4 bits, two bits for the I component and two bits for the Q component. The mapping of the bits into symbols is frequently done in accordance with the Gray code which helps to minimize the number of bit errors occurring for every symbol error. Because Gray-coding is given to a bit assignment where the bit patterns in adjacent symbols only differs by one bit. This code ensures that a single symbol in error likely corresponds to a single bit in error. The rectangular constellation of a Gray-coded unfiltered 16-QAM, 64-QAM and 256-QAM signals are Figure 10. In 256-QAM, every symbol is encoded with 8 bits. Therefore, higher order M-QAM schemes are much more spectrally efficient, however, quite susceptible to noise and fading. As a result, higher order M-QAM schemes are more often used nowadays in cable transmission systems rather than wireless systems where transmission degradation may be worse.

4.2.2.3. QAM demodulation. The information is carried in the phase and amplitude of the modulated carrier for the QAM signal. The receiver is assumed to be able to generate a reference carrier whose frequency and phase are identical to those of the carrier at the transmitter. When the receiver exploits knowledge of the carrier's phase to detect the signals, the process is called demodulation. Figure 11 shows a block diagram of a QAM demodulator.

At the receiver, the received high frequency signal is first down-converted to a lower intermediate frequency (IF) before being further processed. The demodulator performs the majority of its work at an intermediate or baseband frequency. The mixer in the demodulator converts the IF signal to a baseband signal, by multiplying the incoming IF signal with a locally generated carrier reference and the product is passed through a lowpass filter (LPF). The LPF removes the high-frequency components and selects the difference component from the mixer output. These LPFs also perform as matched filters

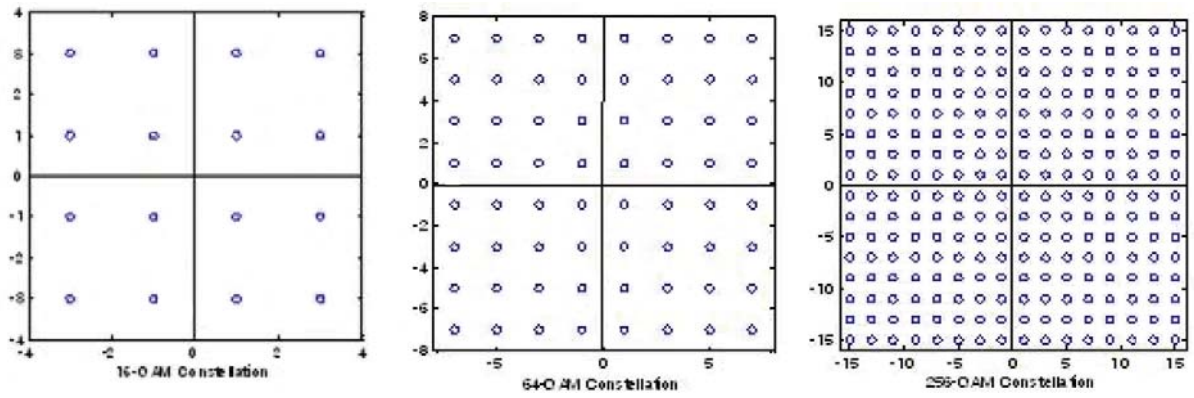

FIGURE 10. 16-QAM, 64-QAM and 256 QAM constellations

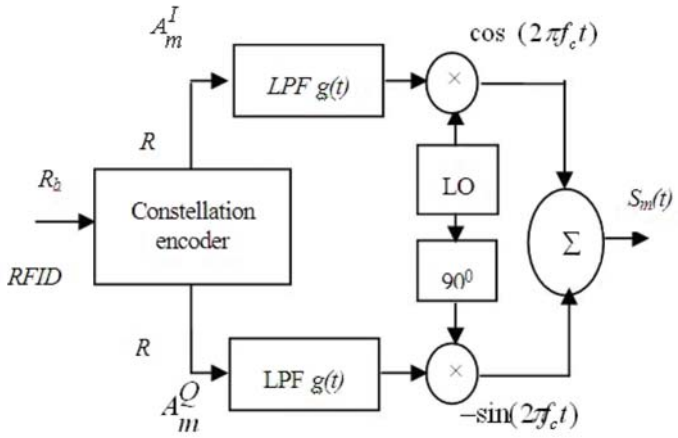

FIGURE 11. Block diagram of a QAM demodulator

whose impulse responses are matched to the transmitted signal to provide the maximum signal-to-noise ratio (SNR) at their output. Assuming that the Gaussian noise is the only channel disturbance, the received signal, $r(t)$, can be expressed as follows.

$$r(t) = s_m(t) + v(t), \tag{22}$$

where $s_m(t)$ denotes the transmitted signal and $v(t)$ refers to the additive noise. Ignoring the noise, $r(t)$ is simplified as follows.

$$r(t) = u_I \cos(2\pi f_c t + \phi_c) - u_Q \sin(2\pi f_c t + \phi_c) \tag{23}$$

where $u_I(t)$ and $u_Q(t)$ are the I and Q amplitudes of the information-bearing signal in which f_c and ϕ_c are the carrier frequency and phase. This signal is demodulated by two quadrature reference carriers as follows.

$$c_I = \cos(2\pi f_o t + \phi_o) \quad \text{and} \quad c_Q = \sin(2\pi f_o t + \phi_o) \tag{24}$$

where f_o and ϕ_o are the frequency and phase of the locally generated carrier. Multiplication of $r(t)$ with $c_I(t)$ followed by lowpass filtering yields the I component as follows.

$$Y_I(t) = \frac{1}{2} u_I(t) \cos[2\pi(f_c - f_o)t + (\phi_c - \phi_o)] - \frac{1}{2} u_Q(t) \sin[2\pi(f_c - f_o)t + (\phi_c - \phi_o)] \tag{25}$$

Similarly, multiplication of $r(t)$ by $c_Q(t)$ followed by lowpass filtering yields the quadrature component.

$$Y_Q(t) = \frac{1}{2} u_Q(t) \cos[2\pi(f_c - f_o)t + (\phi_c - \phi_o)] + \frac{1}{2} u_I(t) \sin[2\pi(f_c - f_o)t + (\phi_c - \phi_o)] \tag{26}$$

It is seen from (26) and (27) that if $f_o = f_c$ and $\phi_c = \phi_o$ the output of QAM demodulator is same as the transmitted baseband signal $u_I(t)$ and $u_Q(t)$; otherwise, the phase error $2\pi(f_c - f_o)t + (\phi_c - \phi_o)$ will reduce the signal level in voltage by the factor $\cos(2\pi[(f_c - f_o)t + (\phi_c - \phi_o)])$ and in power by a factor $\cos^2(2\pi[(f_c - f_o)t + (\phi_c - \phi_o)])$. Also there is cross talk interference from the I and Q components. Since the average power levels of $u_I(t)$ and $u_Q(t)$ are similar, a small phase error causes a large degradation in performance. Hence, the phase accuracy requirements for QAM are very high.

Under ideal operating conditions, the local oscillator (LO) that generates the carrier signal for demodulation at the receiver is identical to that in the transmitter both in frequency and phase. However, obtaining sufficiently stable free-running oscillators in both the transmitter and receiver units is not possible. First of all, the LO at the receiver is generally not synchronous in phase with that at the transmitter. Furthermore, the two oscillators may be drifting slowly with time. A reasonable cost effective crystal oscillator

may have a stability of 1 ppm (part per million) over a given temperature range. If a cellular radio modem operating with a carrier of 1 GHz, the oscillators at each of the link could have a frequency error of $(1 \times 10^6) \times (1 \times 10^9) = 1$ kHz. If both the transmit and receive carrier oscillators begin with the same phase, then, it is expected that the phase error between them to reach 360° after $1 \div 2000 = 0.5$ ms. It is clear that simply achieving a correct starting phase will not allow to ensure adequate coherency for more than a few microseconds. In this application, it is necessary to find a method of correcting the receiver carrier oscillator frequency and phase to match that of the transmitted signal.

4.2.3. *Pilot symbol assisted modulation (PSAM).*

4.2.3.1. PSAM model. Application of QAM for mobile communication in the presence of a rapidly fading channel is challenging because of the amplitude distortion and thus requires high quality channel estimation and equalization. Many researchers [41, 42, 43], have studied PSAM for compensating for the effects of fading at the receiver. We have investigated the different equalization techniques and the effect of pilot symbol spacing and Doppler spread on the performance of PSAM using QAM in this section.

The radio waveforms in transmitter, channel and receiver are defined by SDR program shown in Figure 12. PSAM is used to reduce the effect of channel fading in mobile communication. It tests the channel by periodically inserting known pilot symbols into the data stream. The receiver uses these pilot symbols to determine the channel state information. One of the most important aspects of this procedure is the method used by the receiver to locate timing position of the pilot symbols.

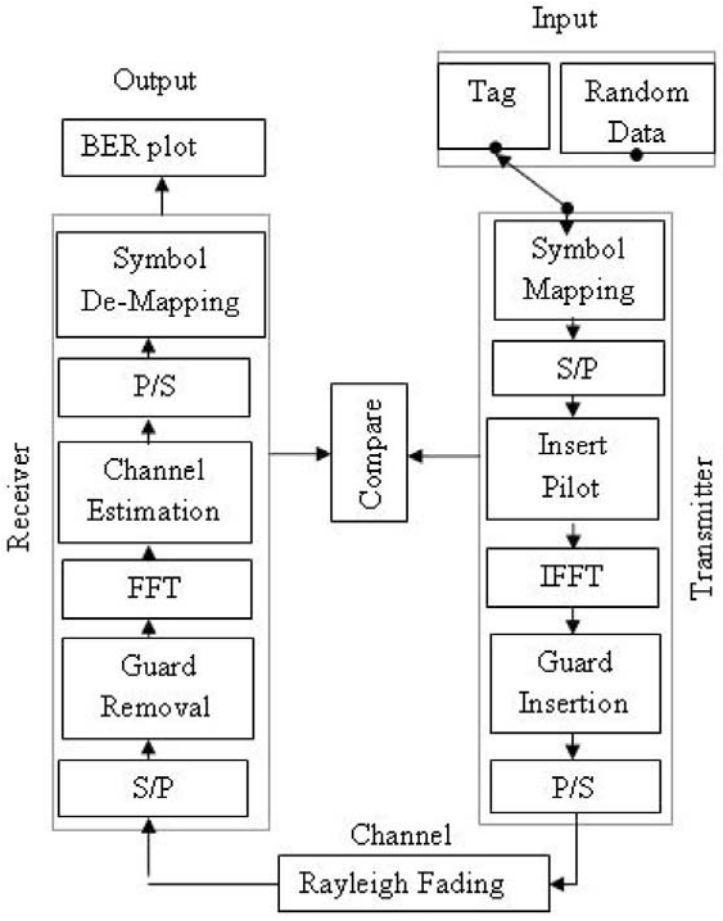

FIGURE 12. Block diagram of PSAM transceiver system

4.2.3.2. PSAM transceiver. The purpose of PSAM transmitter symbol mapping is to map an incoming binary stream of a modulated signals, or data symbols. Once the sequence of binary values has been expressed in complex-valued (Cartesian co-ordinates) form, the next step is to prepare the data signal sequence for conversion to a PSAM waveform by converting the serial data symbol sequence into a number of shorter parallel sequences. Pilot carriers are used in PSAM transmitter to enable the receiver to correct any frequency and timing errors that may cause misalignment between the transmitter and receiver. The IFFT stage is used to create PSAM symbols from the frequency domain waveforms by calculating the IFFT of the input PSAM waveforms. Then, the guard period insertion is appended to the PSAM symbol to ensure that the effects of the previously transmitted symbol have time to dissipate completely before the next symbol is transmitted. Finally, parallel modulated PSAM symbols with pretended guard intervals are then converted to a serial sequence of PSAM symbols, which comprises the real-valued baseband PSAM waveform.

In the PSAM receiver, the information is carried in the phase and amplitude of the PSAM transmitter for the RFID signal. In order to reverse the process of transmission, this serial sequence of received signals must be partitioned into shorter PSAM waveform signals sequences in order to be demodulated. This is the reverse process of parallel to serial conversion stage of PSAM transmitter shown in Figure 12. Then guard period simply removes the pretended which was originally appended to each PSAM symbol of the transmitter. The appended PSAM symbols are extracted back into a frequency domain where FFT is used to convert the real valued of PSAM symbols into frequency domain. Then received signals may have been affected by noise and fading channel. To minimize the possibility of loss of data due to signal degradation, the effects of the channel must be estimated and then using this information, the receiver may then attempt to correct the signal data. The channel estimation and equalization, enables the receiver to compare a known signal sequence with the actual received sequence and then attempt to correct the remaining signal values. After converted the parallel sequence of PSAM symbols into a serial sequence of PSAM symbols, the final stage of PSAM receiver is demapping or demodulation, which is used to recover the original binary information that was transmitted.

5. **Performance Measurement Index.**

5.1. **Bit rate and symbol rate.** To understand and compare different modulation format efficiencies, it is important to understand the difference between bit rate and symbol rate. The signal bandwidth for the communications channel depends on the symbol rate or also known as baud rate. Bit rate is the number of bits that are conveyed or processed per unit of time quantified using the bits per second. Symbol rate is the number of symbol changes made to the transmission medium per second using a digitally modulated signal or a line code measured in baud or symbols/second. The relation between them as follows.

$$symbol\ rate = \frac{Bit\ rate}{Number\ of\ bits\ transmitted\ per\ symbol} \tag{27}$$

5.2. **Bit error rate (BER).** In telecommunication, an error ratio is the ratio of the number of bits, elements, characters, or blocks incorrectly received to the total number of bits, elements, characters, or blocks sent during a specified time interval. The error ratio is usually expressed in scientific notation; for example, 2.5 erroneous bits out of 100,000 bits transmitted would be 2.5 out of 10^5 or 2.5×10^{-5}. BER is a performance measurement that specifies the number of bit corrupted or destroyed as they are transmitted from its source to its destination. Several factors that affect BER include bandwidth, SNR,

transmission speed and transmission medium. Thus, BER can be calculated in an AWGN and one-path Rayleigh fading channels as follows [44, 45, 46, 47].

$$BER_{AWGN} = \frac{1}{2} erfc\left(\sqrt{E_b/N_0}\right) \tag{28}$$

$$BER_{FADING} = \frac{1}{2}\left[1 - \frac{1}{\sqrt{1 + \frac{1}{E_b/N_0}}}\right] \tag{29}$$

where E_b/N_0 is the ration between energy per bit (E_b) and the noise power density (N_0).

5.3. **Signal noise ratio.** In analog and digital communications, signal-to-noise ratio (SNR) is defined as the ratio of a signal power to noise power expressed in decibel (dB). The mathematical expression of SNR is

$$SNR = 10\log_{10}\left(\frac{\text{signal power}}{\text{noise power}}\right) \text{dB} \tag{30}$$

5.4. **Sink detector.** The ultimate task of receivers is to produce an accurate replica of the transmitted symbol sequence. The optimum sink detector is designed to minimize the probability of error in the presence of the system and channel impairments. An important measure of modem performance is the *probability of error*. The probability of the sink detector making an incorrect decision is termed the probability of symbol error. The probability of a symbol error for the M-ary QAM system in the presence of AWGN as a function of E_b/N_0 is obtained as:

$$P_s = 2\left(1 - \frac{1}{\sqrt{M}} efrc\left(\sqrt{\frac{3K}{2\left(M-S\right)}\left(\frac{E_b}{N_0}\right)}\right)\right) \tag{31}$$

where $K = \log_2 M$ and E_b/N_0 denotes the ratio of the bit energy E_b to noise power spectral density N_0. It is an expression of SNR, normalized by bandwidth, B and bit rate, R_b, denoted by

$$\frac{E_b}{N_0} = \frac{S}{N}\left(\frac{B}{R_b}\right) \tag{32}$$

In fact, the user is more concerned with the probability of bit error than symbol error as this directly impinges on the integrity of the data sent to the user. For a RFID system, bit error and symbol error are identical as each symbol error corresponds to a single bit error. Since the error caused solely from AWGN in an adjacent symbol for useful operating levels of E_b/N_0, the detection process mistakes for those adjacent to the correct symbol. When a Gray-coding is used in mapping, we can infer that the bit error probability, P_b, will be given approximately by the symbol error probability, P_s, divided by the number of bits K in each symbol, that is

$$P_b \approx \frac{1}{K} P_s \quad \text{where} \quad K = \log 2M \tag{33}$$

5.5. **Filtering and intersymbol interference of SDR.** Filtering allows the transmitted bandwidth to be significantly reduced without losing the content of the digital data. This improves the spectral efficiency of the signal, as illustrated in Figure 15. On the other hand, filtering results in the symbols spreading in time. This spreading causes part of the symbol energy to overlap with neighbouring symbols, which is called intersymbol interference (ISI). ISI can significantly degrade the ability of the data detector to differentiate a current symbol from the diffused energy of adjacent symbols. This can lead to detection errors and will reduce the BER performance.

To get zero ISI, the overall system filter transfer function must be what is termed a Nyquist frequency response. For this type of filter, the time response goes through zero with a period that exactly corresponds to the symbol spacing. By sampling the symbol sequence at the precise symbol times point, the energy spreading from the adjacent symbols does not affect the value of the present symbol, and ISI is thus eliminated. A commonly used realization of the Nyquist filter is a raised cosine (RC) filter. The impulse response, $h_{RRC}(t)$, and the frequency response, $H_{RRC}(t)$, of the RC filter is given by

$$h_{RC}(t) = \sin\left(\frac{\pi t}{T}\right)\frac{\cos(\pi r t/T)}{1-(\pi r t/T)^2} \tag{34}$$

$$H_{RC}(f) = \begin{cases} T & |f| \le \frac{1-r}{2T} \\ \frac{T}{2}\left[1+\cos\left(\frac{\pi T}{r}\left(|f|-\frac{1-r}{2T}\right)\right)\right] & \frac{1-r}{2T} < |f| \le \frac{1+r}{2T} \\ 0 & \frac{1+r}{2T} < |f| \end{cases} \tag{35}$$

where r is called the roll-factor, which determines the filter bandwidth and takes values in the range $0 \le r \le 1$. It represents a trade-off between the sharpness of the transition band of the filter and the magnitude of the ringing of the impulse response of the filter. T is the symbol period, which is inversely proportional to symbol rate R, i.e., $T = 1/R$. The response of the RC filter is illustrated for five values of r ($r = 0, 0.25, 0.5, 0.75, 1$).

Usually, this RC filter is split equally into a root raised cosine (RRC) filter pair, with one in the transmitter, performing the pulse shaping to constrain the modulated signal bandwidth, and the other in the receiver, performing matched detection for optimizing the SNR of a known signal in the presence of AWGN. The RRC filter is so called because the transfer function is exactly the square root of the transfer function of the RC filter. The impulse response, $h_{RRC}(t)$, and the frequency response, $H_{RRC}(t)$, of the RRC filter is given by

$$h_{RC}(t) = \frac{4r}{\pi\sqrt{T}}\frac{\cos\left[(1+r)\,\pi t/T\right] + \frac{1}{4rt/T}\sin\left[((1-r)\,\pi t/T)\right]}{1-(4rt/T)^2} \tag{36}$$

$$H_{RC}(f) = \begin{cases} T & |f| \le \frac{1-r}{2T} \\ \frac{T}{2}\left[1+\cos\left(\frac{\pi T}{r}\left(|f|-\frac{1-r}{2T}\right)\right)\right] & \frac{1-r}{2T} < |f| \le \frac{1+r}{2T} \\ 0 & \frac{1+r}{2T} < |f| \end{cases} \tag{37}$$

Inspecting these two degradation of RC and RRC (illustrated in Figure 15), we see that they have a similar appearance, but the RRC pulse makes slightly faster degradation, thus its spectrum does not decay as rapidly as the spectrum of the RC pulse. Another important difference is that the RRC pulse does not exhibit zero ISI. However, if RRC filter is used at both the transmitter and the receiver, the product of these transfer functions being a raised cosine, will give rise to an output having zero ISI.

6. **Results.**

The performance of the developed SDR is evaluated by finding BER under various modulations, data communication by sink detector and degradation of Rayleigh facing channel under various roll off factors. The developed SDR is tested under two case studies such as vehicle crash data transmission and image transmission, respectively.

6.1. **Bit error rate.**

The results obtained from the simulations of the PSK, QAM and PSAM modulation systems evaluated under AWGN and Rayleigh fading channels are documented in this paper. As shown in Figure 13, at any target error rate, there are significant gaps between these modulation schemes. For example, at a target error rate of 0.1%, PSK requires 11 dB of SNR. When the channel SNR is at that value, the modulation

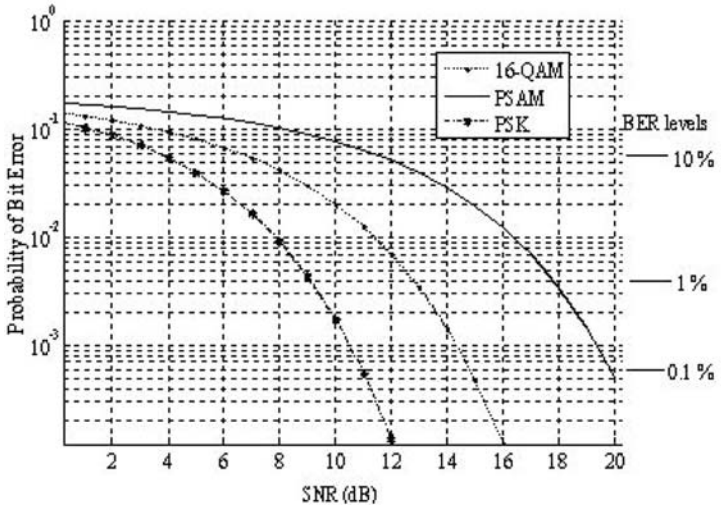

FIGURE 13. BER performance of RFID transceiver in adaptive modulation

achieved 0.1% BER. However, for all values between 11 dB and 12 dB, the modulation used PSK and achieves 0.1% BER. Only when the channel reaches 12 dB and the modulation scheme switches to QAM, the BER returned to the target. Thus, the performance will tend to be better than the target, as shown in Figure 15, except when the SNR is below the value needed for PSK to achieve the target.

As the SNR increased, the spectral efficiency increased, without sacrificing BER performance. Clearly, the target BER cannot be achieved when the SNR is too low (i.e., lower than the required SNR for PSK). However, above that threshold, the target error rate was achieved, and the spectral efficiency increased. The simulated performance matched the theoretical performance very well, with a slight deviation at low BER values. This deviation is likely due to an inadequacy in the statistical sampling of the error process at extremely low error rates. At high SNRs, the spectral efficiency does not achieve 6 bits per symbol for a target BER of 0.1% or 1%, whereas, for the 10% BER, it achieves 6 bits per symbol from 22 dB onwards. For higher target BER values, the transmitter selects PSAM at lower SNRs because it can tolerate a 10% error rate. However, for the other two targets, the modulation schemes fluctuate from PSK to QAM even at a high SNR, maintaining the spectral efficiency at high SNR values. Thus, for each modulation scheme at an average SNR value for different BER targets: it is concluded that a higher target error rate corresponds to a higher utilization of PSAM and a higher spectral efficiency.

6.2. **Sink detector performance.** RFID data communication performance by the sink detector in terms signal to noise ratio through SDR under type of digital modulation schemes on both AWGN and fading channels is shown in Figure 16. In all the cases, the proposed system provides degraded performance in PSAM and QAM, and satisfactory performance in PSK modulations. For a typical SNR value of 4 dB, the BER values for PSK, QAM and PSAM modulations are 0.002035, 0.5086 and 0.7586 respectively. The system performance is improved by 8 to 16 dB. The system shows almost flat degraded performance for a wide value of SNR (4-16 dB). The BER approaches zero above 12 dB SNR for PSK. It is clearly found from the Figure 14 that the system performance for QAM and PSAM degrades compared with PSK using the sink detector.

6.3. **Roll off factor.** The performance degradation of PSAM in the Raleigh fading channel is shown in Figure 15, where the SNR was set to 10 dB. The probability of the performance degradation of PSAM is plotted based on the roll-off factor from 0 to 1, and the

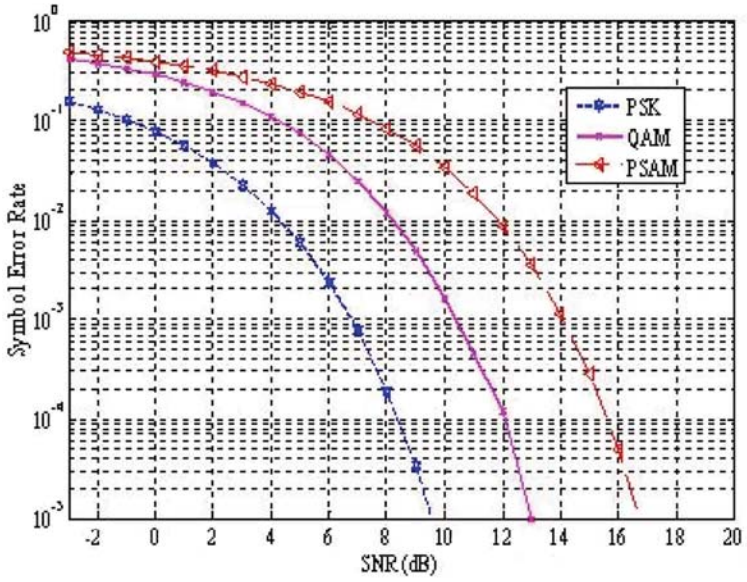

FIGURE 14. Sink performance of various modulation schemes

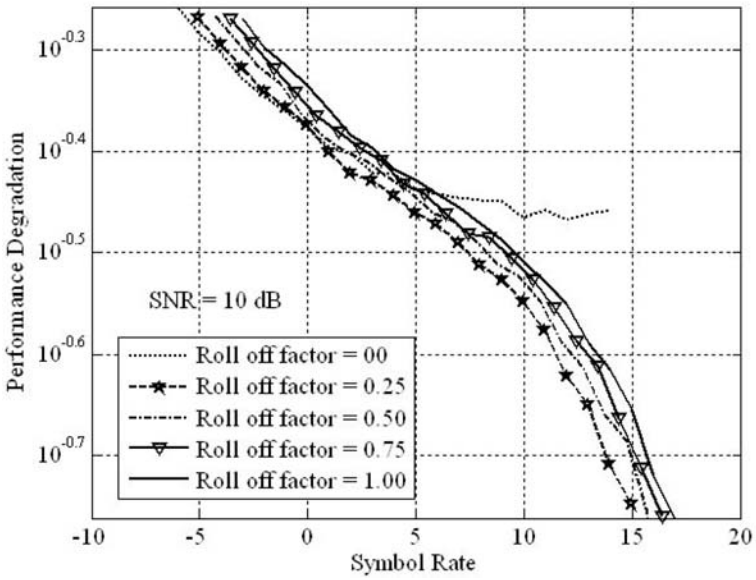

FIGURE 15. Performance degradation of PSAM for different roll-off factors

number of samples per symbol is 16. The acquisition performance degradation was obtained by dividing the probability of the true acquisition under different carrier frequency offset values to the probability of the true acquisition under zero frequency offset. The plot shows that, in the presence of different frequency offsets, PSAM has better performance degradation. It is clear that the simulation results at 10 dB of SNR with large roll-off factor allows for SDR operation with better performance degradation.

6.4. **Case study for vehicle crash data transmission.** A practical approach for determining modulation performance of vehicle crash data using SDR was produced whereby the performance was measured using modulation techniques over an AWGN. Figure 16 shows the vehicle crash data as obtained from a crash generating device [48, 49] in order to transmit wireless signals. Figure 16(a) depicts that the simulation crash velocity of the

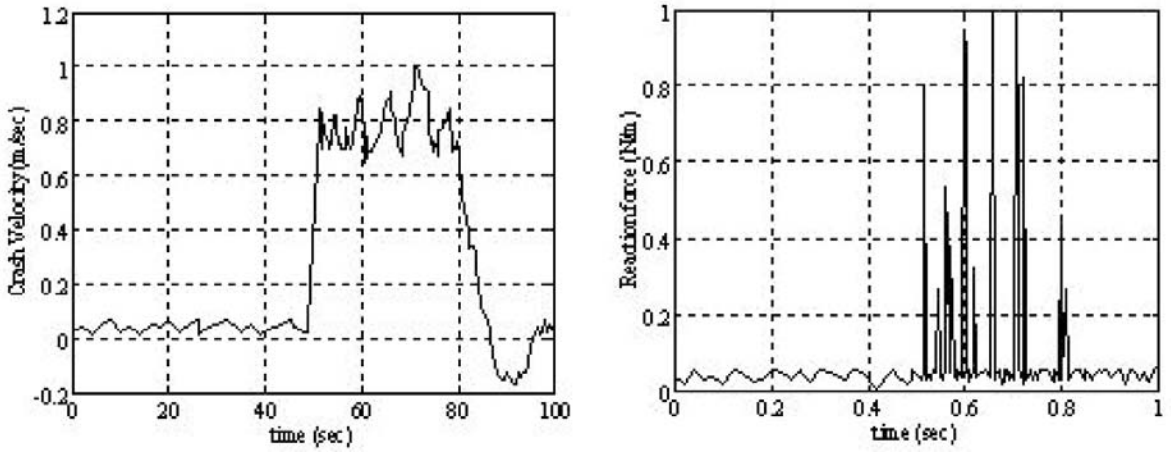

(a) (b)

FIGURE 16. Crash generated data: (a) crash velocity data, (b) reaction force crash data

static vehicle repeated crash response for approximately 50 to 80 seconds. The repeated conduction time for the crash reaction force is 51 to 80 sec as shown in Figure 16(b). Using SDR (explain above), simulations were run to compare performance. The input signal Figure 16(a) is modulated before passing the channel. The transmission channel has several effects on the signal in a physical system. The finite bandwidth of the channel causes distortion in the ideal signal, noise from various sources is also introduced and finally the channel may also attenuate the input signal. Other effects, such as dispersion, may also be present but it is not relevant in this case. The effects of attenuation and noise can be modeled by the addition of Gaussian white noise to the signal, effectively changing the signal to noise ratio at the receiver. The effects of finite bandwidth can be modeled by a simple filter. When the signal is passed through the channel, noise from various sources interferes with the input signal is created. A simple match filter is required to remove the latter noise before demodulation.

Demodulation is a system that attempts to strip the incoming waveform of all the features at the source to facilitate transmission for obtaining a local version of the original time series. In an ideal demodulation system, with perfect equalization and perfect synchronization, all induced side effects of transmission and channel are eliminated. The accuracy of the software defined radio is illustrated in Figure 17 for both crash velocity and reaction force.

6.5. **Case study for image transmission.** Image data or an image file is ideal to test the BER performance and channel effect to signal constellation and give us an intuitive impression and comparison for different channels. In the developed model, PSK, QAM and PSAM modulation is used to modulate the data source. Figure 18(b) is the received image plotted at SNR = 5 dB, it is seen that there are some random noises in the image. However, simulation result show that the received image quality is almost same with the original image in Figure 18(a) at SNR = 10 dB.

Figure 18(c) the BER performance of the simulation result, which is closely identical to theoretical BER, though there is little difference between the BER results. This is reasonable, since the theoretical BER is based on the assumption of the phase information of modulated signal. However, due to the time-variant channel, it has estimation error for phase information. It is noticed that the BER performance is improved dramatically in low SNR, while not in high SNR. This is also reasonable, since in low SNR, white

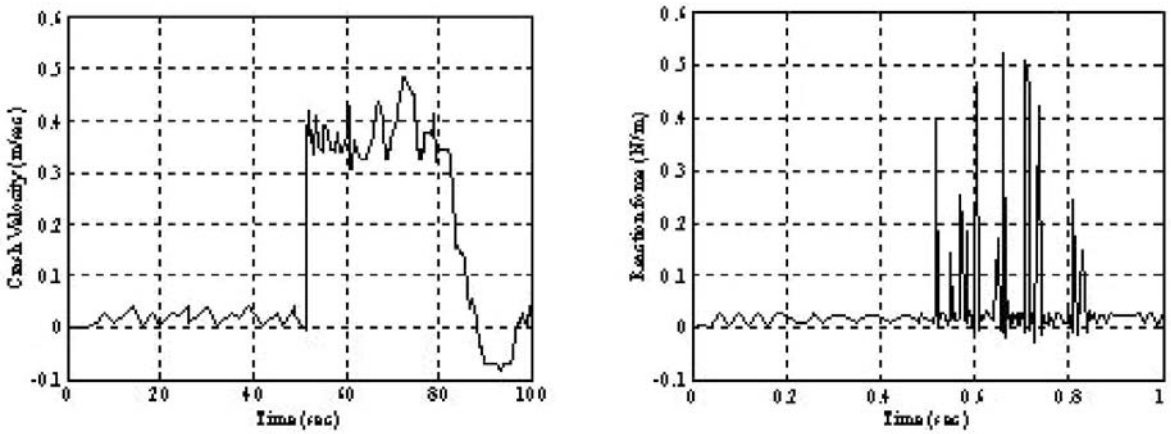

(a) (b)

FIGURE 17. Received signals using SDR: (a) velocity, (b) reaction force

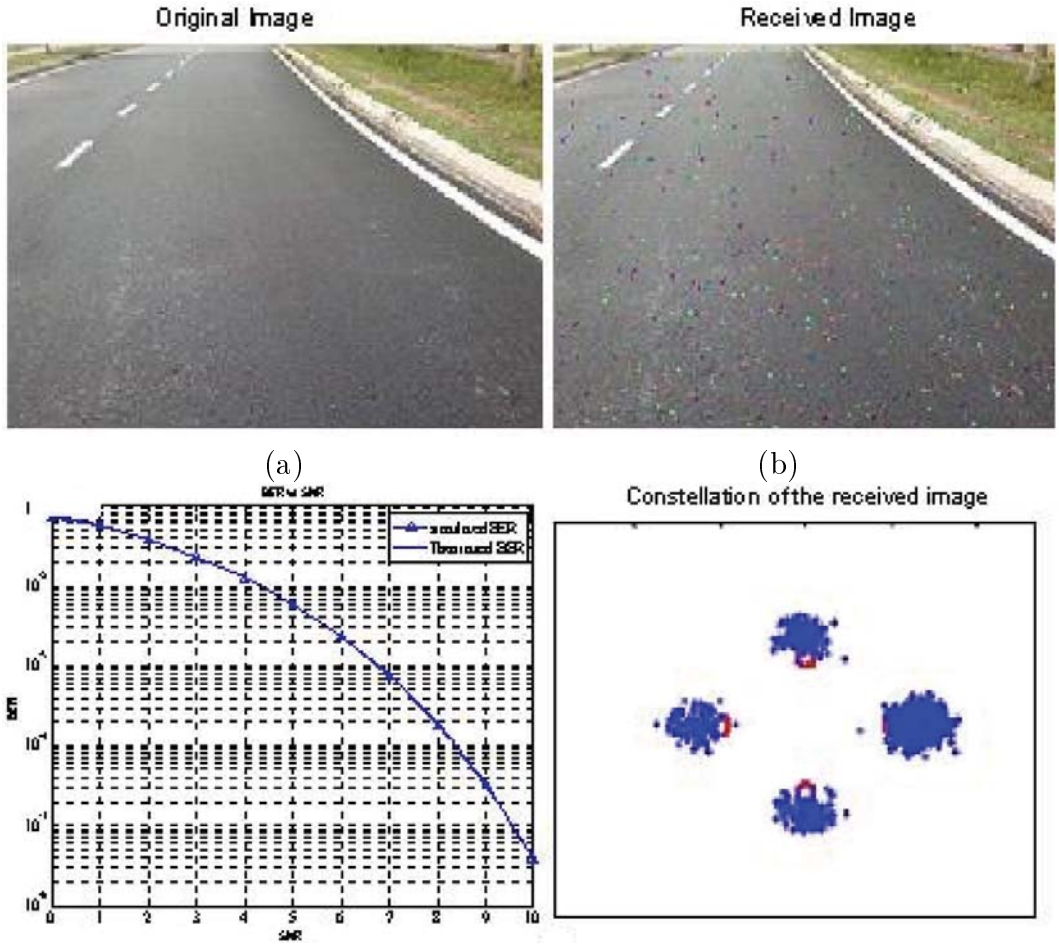

(a) (b) (c) (d)

FIGURE 18. Received image with BER and constellation diagram

Gaussian noise dominate the BER error, which can be improved by enhancing SNR, while in high SNR, phase estimation error dominate the BER error, which cannot be improved by simply enhancing SNR. The constellation is plotted at SNR = 10dB as shown in Figure 18(d), in which both the BER performance and constellation are greatly improved by channel phase estimation.

TABLE 3. Comparison of proposed SDR features with non SDR and existing SDR system

Features	Non SDR system			Existing SDR			
	Cummings et al. [33]	Hatai, Chak [52]	Baines, Pulley [54]	Jignesh et al. [50]	Bhalchandra, Aldar [51]	Ramacher [53]	Proposed SDR system
Bandwidth	5 GHz	15 GHz	6 GHz	2.5 GHz	3 GHz	7 GHz	10 kHz-14.5 GHz
SNR	$\geq$ 25 dB	35 dB	30 dB	20 dB	30 dB	25 dB	0-20 dB
Data Rate (Mbps)	30	12	3	25	20	3	20
Application	Limited application			Video, Image			Wide Application
BER vs (E_b/N_o)	44.7	26.3	21.2	35.6	20.2	18.6	15.2
Reliability	$\geq$ Compare to SDR			Higher			Standard
Hardware Complexity	More Complex	Large Bandwidth	Complex	Simple compare to non SDR	Low Bandwidth	Non-complex	Easy to modify
Hardware Cost	Cost	High	High	less cost	less	less	Very Low
Implement-tion on FPGA	Relatively Complex			Easier implement			Very easy to implement

6.6. **Comparison results.** Optimizing the basic features of proposed SDR system, the reduction of the hardware usage and improvement in the performance has been done. Table 3 summarized the comparison results between the non SDR systems, existing SDR systems and the proposed SDR system, respectively implementing by a direct digital synthesis. Detail features are as follows in Table 3 [33]. Simulations results of the proposed SDR showed that the algorithm improves performance significantly as compared to a non SDR system, fixed modulation system under variable environmental and quality of service requirements. The proposed system improves BER up to 10%, data rate up to 100%, without sacrificing performance of any other parameter. When the qualities of service goals change dynamically, the modulation techniques for RFID transceiver performs significantly better than for a non SDR system goal. The proposed SDR system also improves performance for adhoc and sensor networks by supplementing the MAC protocols to improve BER, energy efficiency, or data rate. Further, it does not increase the hardware cost or complexity of the non SDR transceiver architecture, because it requires changes only to the control logic [50, 51, 52, 53, 55].

7. **Conclusion.** The goal of this paper was to develop and test PSK, QAM and PSAM modulations suitable for programmable SDR and RFID wireless applications where the SNR can vary over a wide range. To meet this goal, a theoretical framework was developed for RFID signals. In this framework, data were generated by a source and then modulated and coded into symbols to be transmitted by TX. Signals passed through channel, where fading and noise were introduced. Transmitted bits were detected at RX and sent to SINK, where the BER result was calculated. This development resulted in a framework that allowed the RFID signal to be modulated with a constellation that was most appropriate for the channel conditions between the source and destination at the point in time when the signal was transmitted. The result is an intelligent reader that reads any tag to

upgrade the system at different frequencies. Therefore, the effects of fading amplitude and phase estimation error on the BER of M-QAM over flat Rayleigh fading and AWGN channels were summarized. The results were obtained by averaging the SNR. Based on the simulation results shown in Section 5, the QAM has the best performance in terms of BER versus SNR in the AWGN channel. In conclusion, in the case when the bit transmission rate is a high requirement, QAM and PSAM can be used as the modulation scheme for better transmission performance. Two case studies have been conducted such as vehicle crash data and image data transmission. The case studies proved that the proposed SDR system greatly influence the performance on data transmission, BER performance and image constellation. Also a comparison is provided between the proposed, non SDR and existing SDR systems to analyze and demonstrates the effectiveness of the proposed SDR performance.

Acknowledgment. The authors would like to thank the Universiti Kebangsaan Malaysian (UKM) for funding this work through research grants UKM-GGPM-ICT-107-2010 and UKM-GUP-08-26-098.

REFERENCES

[1] S. Han, H. Lim and J. Lee, An efficient localization scheme for a differential-driving mobile robot based on RFID system, *IEEE Trans. Ind. Electron*, vol.53, no.5, pp.3362-3369, 2007.

[2] M. Bhuptani and S. Moradpour, *RFID Field Guide Deploying Radio Frequency Identification*, Prentice Hall, New York, 2005.

[3] K. Domdouzis and B. Kumar, Radio-frequency identification (RFID) applications: A brief introduction, *Advanced Engineering Informatics*, vol.21, no.4, pp.350-355, 2007.

[4] K. L. Du and M. N. S. Swamy, *Wireless Communication Systems*, Cambridge University Press, UK, 2010.

[5] J. Bjorkqvist and S. Virtanen, Convergence of hardware and software in platforms for radio technologies, *IEEE Communication Magazine*, vol.44, no.11, pp.52-57, 2006.

[6] M. A. Hannan, A. Hussain, S. A. Samad, A. Mohamed, D. A. Wahab and A. I. Kamal, Development of an intelligent safety system for occupant detection, classification and position, *International Journal of Automotive Technology*, vol.7, no.7, pp.827-832, 2006.

[7] M. Islam, M. A. Hannan, S. A. Samad and A. Hussain, QAM in software defined radio for vehicle safety application, *Australian Journal of Basic and Applied Science*, vol.4, no.10, pp.4904-4909, 2010.

[8] S. Weis and S. Sarma, Security and privacy aspects of low-cost radio frequency identification systems, *Security in Pervasive Computing: The 1st International Conference*, Boppard, Germany, 2004.

[9] M. D. Blech, P. Neumaier, A. T. Ott, A. A. Zan and T. F. Eibert, Performance analysis of a software defined sub-sampling ultra-wideband B-/QPSK impulse radio transceiver, *Proc. of the 2nd European Conference on Wireless Technology*, Rome, Italy, pp.112-115, 2009.

[10] A. Haghighat, A review on essentials and technical challenges of software defined radio, *Proc. of the IEEE Military Communications Conference*, Anaheim, CA, USA, pp.377-382, 2002.

[11] F. Rivet, Y. Deval, J. B. Begueret, D. Dallet, P. Cathelin and D. Belot, A disruptive receiver architecture dedicated to software defined radio, *IEEE Transactions on Circuits and Systems II*, vol.55, no.4, pp.344-348, 2008.

[12] K. Rao, P. Nikitin and S. Lam, Antenna design for UHF RFID tags: A review and a practical application, *IEEE Trans. Antennas Propag*, vol.53, no.12, pp.3870-3876, 2005.

[13] C. Floerkemeier, C. Roduner and M. Lampe, RFID application development with the Accada middleware platform, *IEEE Systems Journal*, vol.1, no.2, pp.82-94, 2009.

[14] S. Preradovic, N. C. Karmakar and I. Balbin, RFID transponders, *IEEE Microwave Mag.*, vol.9, pp.90-103, 2009.

[15] W. H. Tuttlebee, *Software Defined Radio: Enabling Technologies*, Wiley, England, 2002.

[16] S. T. Wang, L. C. Wu, C. Y. Hsu and W. C. Ni, Software downloading in reconfigurable networks of open wireless architecture using SDR technology, *IEEE Communication Magazine*, vol.44, pp.128-134, 2006.

[17] L. B. Michael, M. J Mihaljevic and S. Haruyama, A framework for secure download for software defined radio, *IEEE Communication Magazine*, vol.40, pp.88-96, 2002.

[18] F. F. Digham and M. S. Alouini, Variable-rate variable-power hybrid M-FSK M-QAM for fading channels, *Proc. of the IEEE 58th Vehicular Technology conference*, Orlando, FL, USA, pp.1512-1516, 2003.

[19] H. Gharavi, Pilot-assisted 16-level QAM for wireless video, *IEEE Transactions on Circuits and Systems for Video Technology*, vol.12, no.2, pp.77-89, 2002.

[20] M. Isaka, M. Fossorier, R. M. Zaragoza, S. Lin and H. Imai, Multilevel coded modulation for unequal error protection and multistage decoding – Part II: Asymmetric constellations, *IEEE Transactions on Communications*, vol.48, no.5, pp.774-786, 2000.

[21] M. Islam, M. A. Hannan, S. A. Samad and A. Hussain, Modulation technique for software defined radio application, *Proc. of the 3rd WSEAS international Conference on Circuits, Systems, Signal and Telecommunications*, Ningbo, China, pp.179-182, 2009.

[22] L. V. Subramaniam, S. Rajan and R. Bahl, Performance of 4- and 8-state TCM schemes with asymmetric 8-PSK in fading channels, *IEEE Transactions on Vehicular Technology*, vol.49, no.1, pp.211-219, 2000.

[23] L. Zhou, B. Zheng, J. Cui, S. Xu, B. Geller and A. Wei, Cross layer design for flow control in co-operative multi-hop wireless networks, *International Journal of Innovative Computing, Information and Control*, vol.4, no.11, pp.2977-2986, 2008.

[24] F. F. Digham and M. S. Alouini, Spectrally efficient hybrid FSK/QAM with optimum bit and power loading, *Proc. of the IEEE International Conference on Communications*, Istanbul, Turkey, pp.5022-5027, 2006.

[25] S. G. Klang, Performance of ML modulation classifier for multilevel QAM signals, *Proc. of the IEEE Region 10 Conference (TENCON 2004)*, Thailand, vol.2, pp.292-295, 2004.

[26] Y. S. Kim, C. J. Kim, G. Y. Jeong, Y. J. Bang, H. K. Park and S. S. Choi, New rayleigh fading channel estimator based on PSAM channel sounding technique, *Proc. of the IEEE International Conference on Communications*, Montreal, Canada, pp.1518-1520, 1997.

[27] S. Ohno and G. B. Giannakis, Average-rate optimal PSAM transmissions over time-selective fading channels, *IEEE Transactions on Wireless Communications*, vol.1, no.4, pp.712-720, 2002.

[28] J. Mar, C. C. Kuo, Y. R Lin and T. H. Lung, Design of software-defined radio channel simulator for wireless communications, *IEEE Transactions on Instrumentation and Measurement*, vol.58, no.8. pp.2755-2766, 2009.

[29] J. B Simoneau and L. W. Pearson, Digital augmentation of RF component performance in software defined radio, *IEEE Transactions on Microwave Theory and Techniques*, vol.57, pp.573-581, 2009.

[30] E. Hossain and T. Issariyakul, Performance bound of dynamic forward link adaptation in cellular W-CDMA networks using high-order modulation and multicode formats, *IEEE Electronics Letters*, vol.40, no.2, pp.132-133, 2004.

[31] A. Jamin, P. Mahonen and Z. Shelby, Software radio implementation by wireless LAN's, *Proc. of the 12th Tyrrhenian International Workshop on Digital Communication*, 2000.

[32] T. Shono, Y. Shirato, H. Shiba, K. Uehara, K. Araki and M. Umehira, IEEE 802.11 wireless LAN implemented on software defined radio with hybrid programmable architecture, *IEEE Transactions on Wireless Communications*, vol.4, no.5, pp.2299-2308, 2005.

[33] M. Cummings and S. Haruyama, FPGA in the software radio, *IEEE Communications Magazine*, vol.37, no.2, pp.108-112, 1999.

[34] H. F. Harmuth, A generalized concept of frequency and some applications, *IEEE Transactions on Information Theory*, vol.14, no.3, pp.375-382, 2003.

[35] M. Wasserman, SDR-based readers keep pace with changing RFID technology, *RTC Magazine*, pp.42-45, 2007.

[36] R.-C. Wang, W.-S. Juang and C.-L. Lei, A robust authentication scheme with user anonymity for wireless environments, *International Journal of Innovative Computing, Information and Control*, vol.5, no.4, pp.1069-1080, 2009.

[37] H. Arsalan, *Software Defined Radio, and Adaptive Wireless Systems*, Springer, University of South Florida, FL, USA, 2007.

[38] A. A. Tabassam, F. A. Ali, S. Kalsait and M. U. Suleman, Building software-defined radios in MATLAB simulink – A step towards cognitive radios, *Proc. of the 13th International Conference on Computer Modeling and Simulation*, Cambridge, UK, pp.492-497, 2011.

[39] K. B. Alison, Dynamically reconfigurable software defined radio for GNSS applications, *Proc. of the SDR 2010 Technical Conference and Product Exposition*, CO, USA, 2010.

[40] A. Karmakar and A. Sinha, A novel architecture of a reconfigurable radio processor for implementing different modulation schemes, *Proc. of the 3rd International Conference on Computer Research and Development*, Shanghai, China, pp.115-119, 2011.

[41] C. Yunfei and N. C. Beaulieu, Optimum pilot symbol assisted modulation, *IEEE Transactions on Communications*, vol.55, no.8, pp.1536-1546, 2007.

[42] M. Dong, L. Tong and B. M. Sadler, Optimal insertion of pilot symbols for transmissions over time-varying flat fading channels, *IEEE Transactions on Signal Processing*, vol.52, no.5, pp.1403-1418, 2004.

[43] T. A. Chen, M. P. Fitz, S. Li and M. D. Zoltowski, Two-dimensional space-time pilot-symbol assisted demodulation for frequency-nonselective rayleigh fading channels, *IEEE Transactions on Communication*, vol.52, no.6, pp.953-963, 2004.

[44] J. Bellorado, S. Ghassemzadeh and A. Kavcic, Approaching the capacity of the MIMO rayleigh flat-fading channel with QAM constellations independent across antennas and dimensions, *IEEE Transactions on Wireless Communications*, vol.5, no.6, pp.1322-1332, 2006.

[45] M. Takahashi, Self-repairing and adaptive control of MIMO system with faulty sensors, *International Journal of Innovative Computing, Information and Control*, vol.5, no.10(B), pp.3573-3582, 2009.

[46] M. Matsubara, H. Fujimoto, J. Morita and S. Sugimoto, Prefiltering based on world's decomposition for linear MIMO system identification, *International Journal of Innovative Computing, Information and Control*, vol.5, no.1, pp.41-55, 2009.

[47] S. Bernard, *Digital Communications: Fundamentals and Applications*, 2nd Edition, Prentice-Hall, 2001.

[48] A. Hussain, M. A. Hannan, A. Mohamed, H. Sanusi and A. K. Ariffin, Vehicle crash analysis for airbag deployment decision, *International Journal of Automotive Technology*, vol.7, no.2, pp.179-185, 2006.

[49] M. A. Hannan, A. Hussain, A. Mohamed and S. A. Samad, Development of an embedded vehicle safety system for frontal crash detection, *International Journal of Crashworthiness*, vol.13, no.5, pp.579-587, 2008.

[50] O. Jignesh, Y. Patel, P. Trivedi, N. Ranpura, Z. Patel, U. Dalal, R. Jani and S. R. Vijay, Optimized configurable architecture of modulation techniques for SDR applications, *Proc. of the International Conference on Computer and Communication Engineering*, Kuala Lumpur, Malaysia, 2010.

[51] B. G. Bhalchandra and S. D. Aldar, Performance improvement by changing modulation methods for software defined radios, *International Journal of Advanced Computer Science and Applications*, vol.1, no.6, pp.72-79, 2010.

[52] I. Hatai and I. Chakrabarti, FPGA implementation of a digital FM modem for SDR architecture, *Proc. of the 4th International Conference on Computer and Devices for Communication*, Kolkata, India, pp.1-4, 2009.

[53] U. Ramacher, Software-defined radio prospects for multi-standard mobile phones, *Computer*, vol.40, no.10, pp.62-69, 2007.

[54] R. Baines and D. Pulley, A total cost approach to evaluating different reconfigurable architectures for baseband processing in wireless receivers, *IEEE Communications Magazine*, vol.41, no.1, pp.105-113, 2003.

[55] A. J. Goldsmith and S. G. Chua, Variable-rate variable power MQAM for fading channels, *IEEE Transactions on Communication*, vol.45, pp.1218-1230, 1997.